Journal Pre-proof

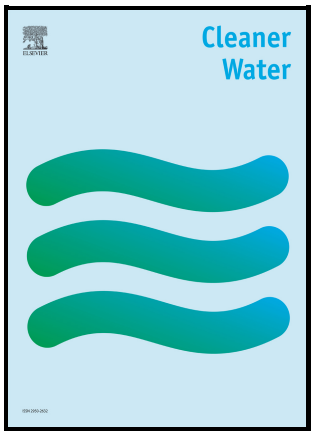

The ability of subsurface dams to protect freshwater abstraction wells against seawater intrusion in heterogeneous aquifers

Antoifi Abdoulhalik, Ismail Abd-Elaty, Ashraf A Ahmed

PII: S2950-2632(25)00036-5

DOI: https://doi.org/10.1016/j.clwat.2025.100098

Reference: CLWAT100098

To appear in: *Cleaner Water*

Received date: 11 December 2024
Revised date: 26 June 2025
Accepted date: 10 July 2025

Please cite this article as: Antoifi Abdoulhalik, Ismail Abd-Elaty and Ashraf A Ahmed, The ability of subsurface dams to protect freshwater abstraction wells against seawater intrusion in heterogeneous aquifers, *Cleaner Water,* (2025) doi:https://doi.org/10.1016/j.clwat.2025.100098

This is a PDF file of an article that has undergone enhancements after acceptance, such as the addition of a cover page and metadata, and formatting for readability, but it is not yet the definitive version of record. This version will undergo additional copyediting, typesetting and review before it is published in its final form, but we are providing this version to give early visibility of the article. Please note that, during the production process, errors may be discovered which could affect the content, and all legal disclaimers that apply to the journal pertain.

© 2025 Published by Elsevier.

Journal Pre-proof

The ability of subsurface dams to protect freshwater abstraction wells against seawater intrusion in heterogeneous aquifers

Antoifi Abdoulhalik[1], Ismail Abd-Elaty[2], Ashraf A Ahmed[1*]

[1] Department of Civil and Environmental Engineering, Brunel University London, Kingston Lane Uxbridge UB83PH, United Kingdom

[2] Department of Water and Water Structures Engineering, Faculty of Engineering, Zagazig University, Zagazig 44519, Egypt.

Corresponding author: ashraf.ahmed@brunel.ac.uk

Abstract

The main purpose of this study was to examine the ability of subsurface dams to protect freshwater abstraction against seawater intrusion in both homogeneous and layered aquifers. Laboratory experiments were conducted in a synthetic aquifer where a subsurface dam was simulated in a homogeneous scenario (case H), and in another scenario where a top low-permeability (low-K) layer was placed in the upper part of the aquifer (case LH). We then conducted numerical simulations using the SEAWAT model to validate the experimental results. We also examined other numerical cases where a low-K layer existed at the middle (case HLH) and the bottom of the aquifer (case HL). The existence of a low-K layer has generally delayed the upconing, and it took longer for the SWI to contaminate the abstraction well. The top low-K layer needed 52% more pumping than the homogeneous aquifer for the wedge to spill over the dam into the landward side. The clean-up time varied substantially from one case to another, with the case HL taking longer than the other cases for SWI removal. The cleanup time was reduced by 23% in the presence of a top low-K layer compared to the homogeneous aquifer. The study demonstrates that a low-K layer on the top of the aquifer contributed positively to improving the ability of the subsurface dams to obstruct SWI, limit saltwater upconing and, therefore, allow more optimal freshwater abstraction. A feature of this study was that it examined the ability of dams to prevent seawater intrusion in the presence of

freshwater pumping, which has not been investigated in previous studies, at least in laboratory experiments.

Keywords:
Saltwater intrusion; Subsurface barriers; Freshwater pumping; Saltwater upconing; Cleaner water.

1 Introduction

Coastal aquifers represent an important source of freshwater for millions living near the coast. However, these aquifers face the threat of being contaminated by seawater intrusion (SWI), which happens naturally because of the density contrast between seawater and freshwater. Controlling factors such as over-abstraction, drought, and sea-level rise further exacerbate the SWI process (Ketabchi et al., 2016). The contamination of groundwater reservoirs and the abandonment of production wells are among the main negative consequences of SWI (Werner et al., 2013; Abdoulhalik et al., 2022a,b). Predicted population rise in coastal areas (Yu et al., 2019), as well as sea level rise (Abdelgawad et al., 2019; Abd Elaty et al., 2024), will further deteriorate coastal aquifers around the globe.

Practical methods have been proposed to preserve coastal groundwater reservoirs from SWI. The most common methods involved decreasing freshwater abstraction (Ketabchi et al. 2016), changing the pumping well locations (Chistelis et al. 2019; Abdelgawad et al. 2018), creating positive hydraulic barriers (Luyun et al., 2011; Shi et al., 2020), pumping out saline water,

which is known as negative hydraulic barriers (Pool and Carrera, 2010), constructing underground barriers (Kaleris and Ziogas, 2013; Abdoulhalik and Ahmed, 2017a, b). Combining the above methods (Elbeling et al., 2019) and injecting compressed air has shown promising outcomes (Zang and Li, 2021; Zang et al., 2023).

1.1 Hydraulic barriers and other methods to control SWI

Elbeling et al. (2019) investigated the potential of using mixed hydraulic barriers for SWI control. Their findings indicated that the negative barrier in such systems had limited effectiveness in remediating coastal aquifers contaminated by SWI. Li et al. (2022) evaluated the performance of injection wells for freshwater recharge in combating seawater intrusion along the California coast. The findings indicated that strategically located injection wells effectively mitigated seawater intrusion, highlighting the importance of site-specific planning and management.

Strack et al. (2016) presented a different method to control seawater intrusion. They suggested that reducing the permeability of the upper part of the aquifer would control SWI and, hence, protect the freshwater reservoirs. However, the experimental investigation carried out by Abdoulhalik et al. (2022b) demonstrated that this method is only effective when lowering the permeability of the upper half of the aquifer thickness, which is impractical and economically very costly.

1.2 Physical Barriers to Control SWI

Amongst the other strategies employed in practice is physical subsurface barriers. Such a physical barrier system was used in various countries, including the Middle East, India, China, and Japan (Stevanović, 2016). Physical barriers can be a cutoff wall, subsurface dams, or a combination of both. The cutoff wall barrier is installed in the upper part of the aquifer and should obstruct the seawater wedge to prevent it from intruding further into the landward side

(e.g. Luyun et al., 2011; Abdoulhalik and Ahmed, 2017a). Subsurface dams are low-permeability barriers that obstruct the lower part of the aquifer while enabling the seaward discharge of freshwater over the tip of the dam, i.e., in the upper part of the aquifer (Abdoulhalik and Ahmed 2017b; Zhang et al. 2021; Abd-Elaty et al., 2024), as shown in Figure 1. This mixed physical barrier combines a cutoff wall and subsurface dams (e.g., Emara et al. 2024; Abdoulhalik et al. 2024).

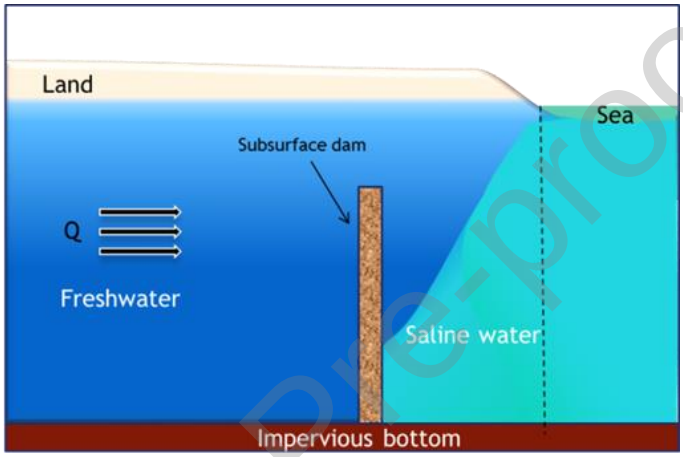

Figure 1. Simplified diagrams of a subsurface dam installed in a coastal aquifer

Recent studies have highlighted the efficiency of subsurface dams in mitigating saltwater intrusion and preserving freshwater resources. For instance, research by Zhang et al. (2021) in the Pearl River Delta, China, demonstrated that subsurface dams effectively reduced the seawater intrusion wedge by up to 70% and saved fresh groundwater reservoirs. Similarly, an investigation by Zheng et al. (2023) found that the aquifer anisotropy affects the height and location of the subsurface dam. Larger horizontal anisotropy led to greater freshwater flow, resulting in a reduced seawater wedge and a shorter subsurface dam. Fang et al. (2021) found that the minimum effective height of subsurface dams was lower in tides compared to non-tidal conditions.

Previous studies showed that layered structures of aquifers significantly impact the performance of subsurface dams in controlling SWI. Specifically, Abdoulhalik and Ahmed

(2017b) showed that subsurface dams performed better in removing residual saline water when a low-permeability layer is at the top of the aquifer; however, the performance worsens when the low-permeability layer is at the bottom of the aquifer. The underlying low-permeability layer slows the freshwater flow and reduces its velocity, impacting the ability to repulse the seawater wedge. None of the studies examining physical barrier performance in heterogeneous media incorporated freshwater abstraction, which is well-known to impose a completely different hydrodynamic condition and produce a saltwater upconing mechanism (Abdelgawad et al. 2018), whereby the freshwater-saltwater transition zone rises below the vicinity of the well. Contamination occurs after 1% of seawater has penetrated the wellbore (WHO, 2011).

1.3 Research gap and study innovation

While several studies investigated the performance of subsurface dams in preventing seawater intrusion, none of them, at least experimentally, have incorporated freshwater pumping conditions when evaluating subsurface dam performance. In addition, no previous studies have attempted to examine how layered heterogeneity would impact the ability of subsurface dams to protect groundwater abstraction in coastal aquifers. This study addressed these two research gaps. Therefore, the main purpose of this study was to examine how typical layered heterogeneity would impact the capability of subsurface dams to prevent the salinisation of pumping wells via a saltwater upconing mechanism.

The study first simulated the saltwater upconing process in a laboratory-scale coastal aquifer model with a subsurface dam in a homogeneous setting, referred to hereafter as the base case or case H, and then with a layered aquifer setting where a low permeability layer overlays the aquifer, referred to hereafter as case LH. The MODFLOW family SEAWAT model was then used to validate results and examine the impact of other layered scenarios on SWI advancement and retreat during freshwater abstraction.

Materials and methods

2.1. Experimental methods and procedure

The experiments were conducted using a laboratory-scale aquifer model of dimensions 0.38 m × 0.15 m × 0.01 m (Figure 2). The tank's thinner thickness allows light to pass through, which is needed for the salt concentration and pixel light intensity calibration process, which is explained below. Clear glass beads, with diameters of 1325 µm (K=108 cm/min) for the aquifer and 780 µm (36 cm/min) for the low K layer, were used to simulate the porous medium.

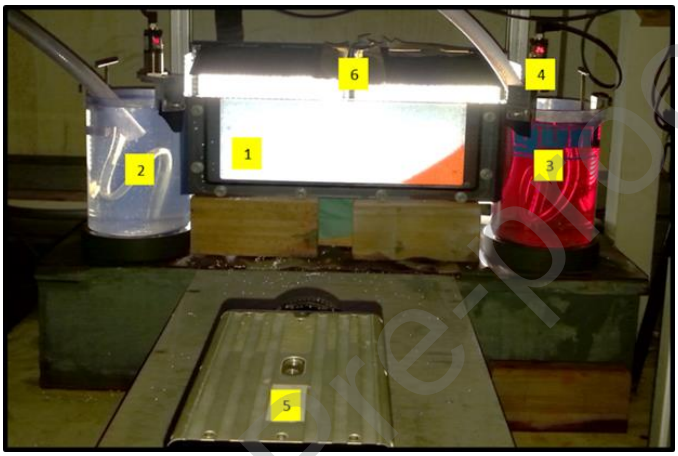

Figure 2: Laboratory set-up; 1) central chamber; 2) freshwater side (water head=135.7mm); 3) saltwater side (water head=129.7mm); 4) sensors; 5) camera; 6) Background lights

The subsurface dam was 12 mm wide, 46 mm high, and was located 50 mm away from the saltwater boundary. As explained in Abdoulhalik et al. (2017, 2024), the dam was made from an impermeable material, plasticine. The effect of the subsurface dam was examined within two aquifer settings, including one homogeneous case and a heterogeneous case, where a low K layer of thickness 45 mm was overlying the aquifer. The thickness of the low K layer accounted for nearly a third of the homogeneous aquifer thickness (h=136 mm). Figure 3 shows the schematic design of the two investigated cases, and Table 1 summarises the main parameters.

Tap water was poured into the left-side reservoir to impose a freshwater head boundary, and dyed saline water was versed into the right-side reservoir to impose a saltwater head boundary condition. The saltwater density was 1025 kg/m^3 and monitored using a hydrometer H-B Durac plain-form polycarbonate. The water level in both reservoirs was accurately monitored with

ultrasonic sensors throughout the experiment. LED lights illuminated the porous medium from behind, and an IDT MotionPro X-Series camera was used to photograph the SWI experiments.

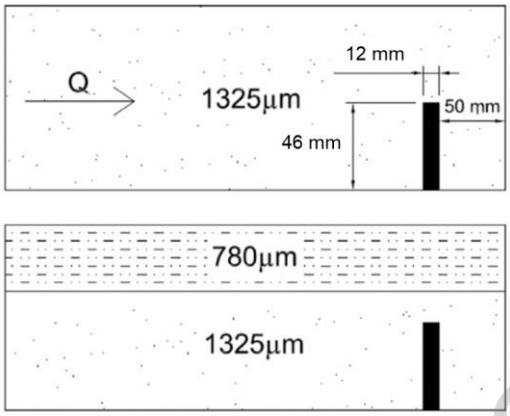

Figure 3. **Schematic design of the investigated cases in the laboratory: the base case (top) and case LH (bottom)**

The pumping well was 85 mm above the aquifer bottom and 190 mm from the seaside boundary. This location was selected based on previous studies (e.g. Abdelgawad et al. 2018; Abdoulhalik et al. 2022). After setting the initial head boundary condition, allowing saltwater penetration into the system (dh = 135.7–129.7 = 6 mm), the pump was turned on, and the abstraction rate was increased incrementally using a 0.1 mL/s incremental step. After each increment, the system was allowed to reach a steady state condition. The first pumping rate was set to 0.09 mL/s, which was incrementally increased by 0.1 mL/s until it reached 0.39 mL/s, the rate that forced saltwater upconing for most tested scenarios and the seater reached the well.. The pump was thereafter switched off to allow the retreat of the saltwater back to the seaside boundary. Full details of the experimental methodology can be found in Abdoulhalik et al. (2022a), Abdelgawad et al. (2018), and Robinson et al. (2016).

2.2. Numerical model and procedure

The SEAWAT code (Guo and Langevin, 2002) was adopted for the validation. The variable density flow (VDF) process solves the variable density flow equation regarding the freshwater head [Guo and Langevin, 2002] Eqs. 1:

$$\nabla\left[\rho\frac{\mu_o}{\mu}K_o\left(\nabla h_0+\frac{\rho-\rho_o}{\rho_o}\nabla z\right)\right]=\rho S_{s,0}\left(\frac{\partial h_o}{\partial t}\right)+\theta\left(\frac{\partial\rho}{\partial C}\right)\left(\frac{\partial C}{\partial t}\right)-\rho_s q^{\backslash}{}_s \quad \ldots\ldots [1]$$

The Integrated MT3DMS Transport (IMT) process solves the solute transport equation ((Zheng and Wang 1999), Eqs. 2:

$$\left(1+\frac{\rho_b K^k{}_d}{\theta}\right)\left(\frac{\partial(\theta C^k)}{\partial t}\right)=\nabla\left[\theta\left(D_m{}^k+\alpha\frac{q}{\theta}\right).\nabla C^k\right]-\nabla.(qC^k)-q^{\backslash}{}_s * C^k{}_s \quad \ldots. [2]$$

Where, ρ_0: fluid density at the reference concentration and temperature; μ: dynamic viscosity; K_0: hydraulic conductivity; h_0: hydraulic head, ρb: bulk density, ρs: density of the solid, S_s: specific storage, t: time; θ: porosity; C: salt concentration, q: specific discharge, q\s: a source or sink, $D^k{}_m$: is the molecular diffusion coefficient for species k; α: is the dispersivity tensor; $K^k{}_d$: distribution coefficient of species k, C_k: the concentration of species k, $C^k{}_s$: the source or sink concentration.

A uniform-size mesh of 0.2 cm was used to discretise the model domain. The cells at the location of the subsurface dam were inactivated. The longitudinal dispersivity was set to 0.1 cm, and the transverse dispersivity value was set to 0.05 cm. The Peclet number criterion was satisfied to ensure numerical stability (Voss and Souza, 1987). The saltwater head boundary (C = 36.16 g/L) was simulated on the right-side boundary, and a freshwater head boundary (C = 0 g/L) was simulated on the left-side boundary.

Table 1. Summary of the numerical parameters (lab-scale)

Input Parameters	Value
Aquifer parameters	
Domain length (cm)	38
Domain height (cm)	13.6
Element size (cm)	0.2

Journal Pre-proof

Journal Pre-proof

Input Parameters	Value
Hydraulic Conductivity (cm/min)	85
Porosity	0.3
Longitudinal dispersivity (cm)	0.1
Transversal dispersivity (cm)	0.01
Freshwater density (kg/m^3)	1000
Saltwater density (kg/m^3)	1025
Freshwater head (mm)	135.7
Saltwater head (mm)	129.7
Well configuration	
Well distance, L_w (cm)	19.0
Well depth, Z (cm)	8.5
Abstraction rates (mL/s) (cm^3/s)	0.09, 0.19, and 0.29
Subsurface dam configuration	
Dam location L (cm)	5.0
Dam height, H (cm)	4.6
Dam thickness (cm)	1.2
Dam hydraulic conductivity (cm/min)	0.0001

The first stress period was used to set the first steady state condition (dh = 135.7–129.7 = 6 mm), whereby saline water penetrated a fully fresh aquifer. The pumping well was simulated in the following stress periods, with an initial abstraction rate of 5.4 cm^3/min (0.09 mL/s). The abstraction rate was then gradually increased using a constant incremental step of 6 cm3/min (0.1 mL/s). The pumping was stopped after saltwater upconing was reproduced. A summary of the numerical parameters used in the simulations is also shown in Table 1. The model scenarios were developed using the pumping well rates of three cases, as in Table 1.

3. Results and discussion

3.1. Experimental model

3.1.1. Advancing-wedge phase: pumping condition

Figure 4 presents the concentration maps of the experiments before the spillage in the base case and case LH. Saline water entered the aquifer after the freshwater level was lowered to 135.7 mm to establish the initial head difference dh = 6 mm. In both cases of homogeneous and layered aquifers, the saltwater wedge built up on the seaward side of the subsurface dam without spilling over the dam. The height of the saltwater wedge along the right boundary was shorter in case LH, with a visibly wider transition zone. After the system reached a steady state condition, the pump was turned on with a pumping rate of Q_1 = 0.09 mL/s, which caused further building up of saline water without causing spillage on the landward side of the wall. The system was left to remain for at least 25-30 minutes to ensure no spillage would eventually occur. The observations showed that while the saline water exceeded the tip of the wall in the base case, the saltwater remained behind the wall in the case of LH and did not reach its top edge.

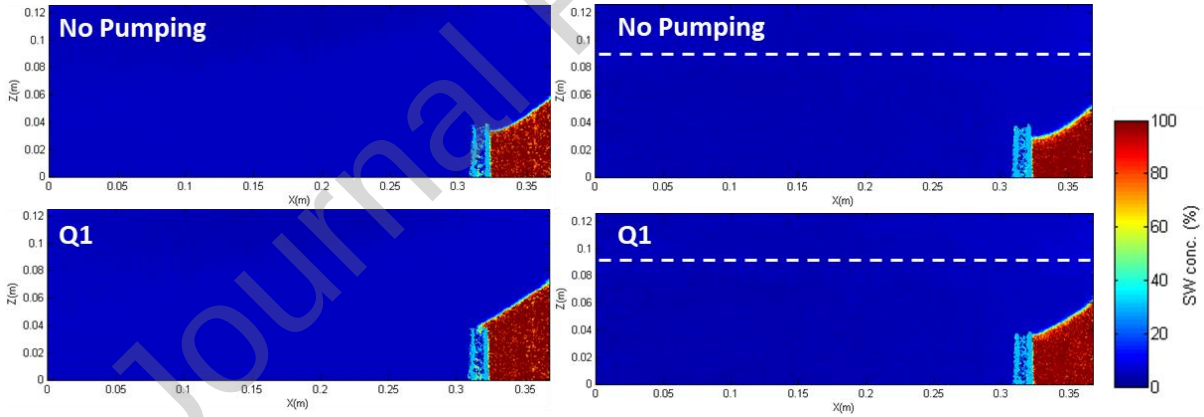

Figure 4: Concentration colour map of the transient **experimental** saltwater wedge before pumping (top images) and under pumping conditions Q=0.09 mL/ (bottom images) in the base case (left) and case LH (right). The dashed line represents the lower boundary of the low-K layer.

The increment of the pumping rate to Q_2=0.19 mL/s caused the saline water to spill over the wall in the homogeneous case, as shown in Figure 5. The spillage occurred within the first 5 minutes following the pumping rate increment, and the intruding wedge continued its landward progression. The freshwater-saltwater transition zone appeared to curve slightly outward under the pumping effect but remained stable until the system reached a steady state (within 70 min).

At this stage, the density contrast effects could withstand the impact of the abstraction, thereby stabilising the wedge below the well without causing salinisation. In the case of LH, increasing the pumping rate did not cause spillage of saline water even after 70 minutes.

Instead, the saltwater wedge continued to build up on the seaward side of the subsurface dam, where it reached a steady state, with the freshwater-saltwater transition zone exceeding the upper edge of the wall. While an abstraction rate Q_2 = 0.19 ml/s could cause saltwater to spill over the subsurface dam in the base case, this pumping rate was insufficient in case LH, suggesting that the low-K layer improved the ability of the subsurface dam to obstruct the SWI and therefore allowed more optimal freshwater abstraction without enabling saltwater to spill over the wall.

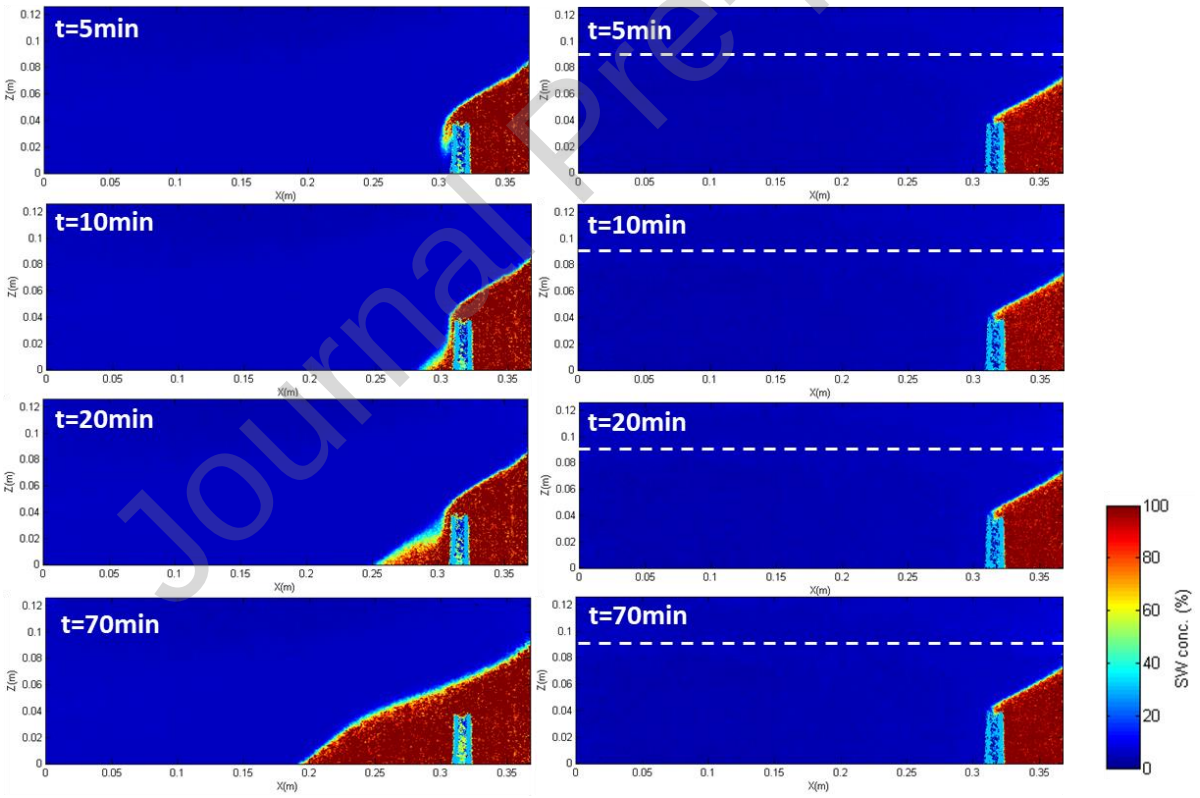

Figure 5: Concentration colour map of the transient **experimental** saltwater wedge under pumping conditions Q= 0.19 mL/s in the base case (left) and case LH (right). The dashed line represents the lower boundary of the low-K layer.

Figure 6 shows the temporal evolution of the saltwater wedge response to freshwater abstraction rate Q = Q_3 = 0.29 ml/s. In the base case, the further increment of the abstraction rate caused

the upward lifting of the saltwater wedge towards the well. The saltwater upconing mechanism eventually started in the first 20 minutes following the pumping rate change, whereby laboratory observations show that low-concentration saline water reached the well. The upconing mechanism reached a steady state within 25 min. In case LH, the further increase of the pumping rate to Q_3 = 0.29 mL/s was sufficient to prompt the saline water to spill over the subsurface dam within the first 5 minutes and continue its progression on the landward side of the wall. This means case LH needed 52% more pumping than the base case for the wedge to spill over the dam into the landside.

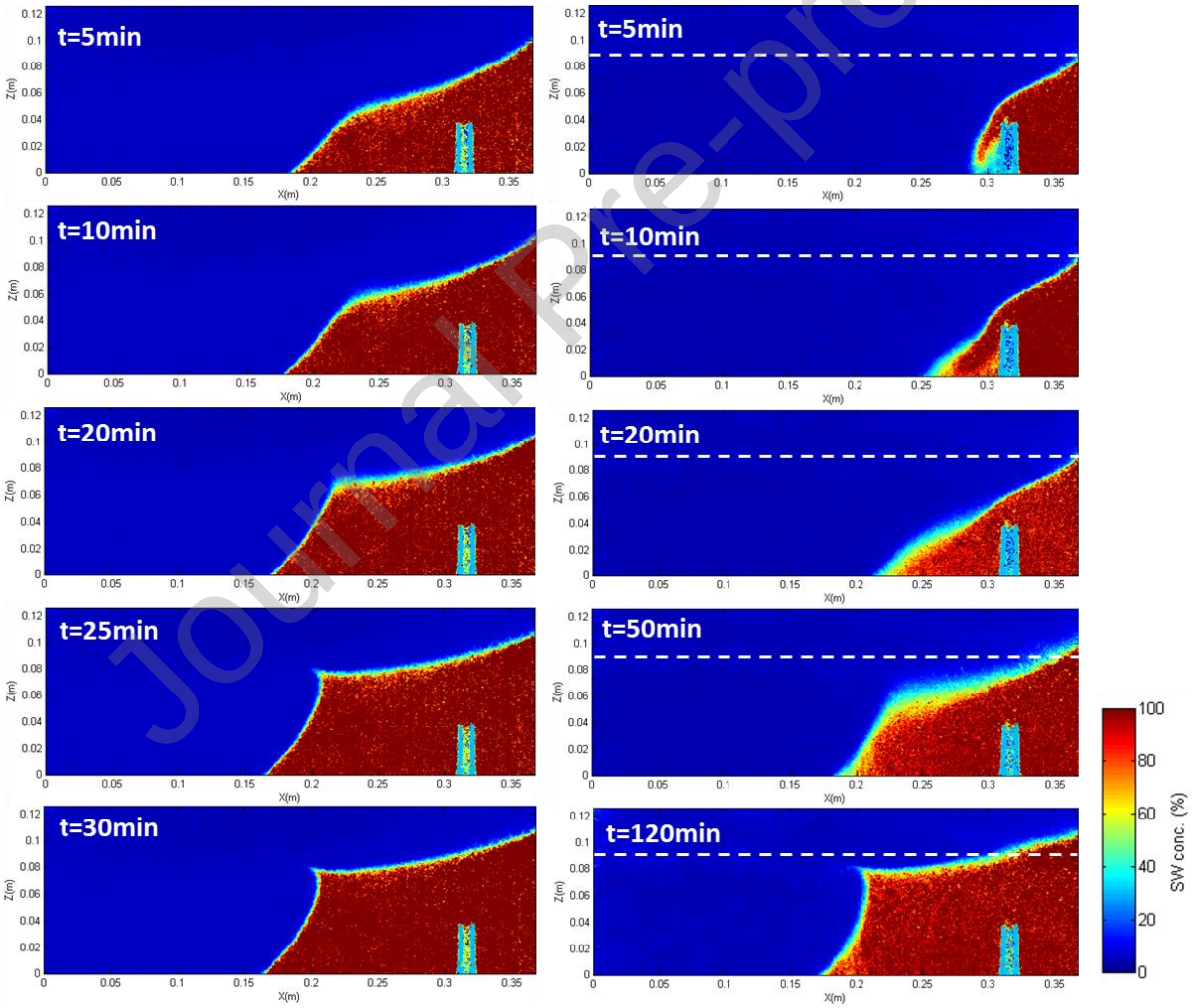

Figure 6: Concentration colour map of the transient **experimental** saltwater wedge under pumping conditions Q3=0.29 mL/s in the base case (left) and case LH (right). The dashed lines represent the lower boundary of the low-K layer.

For case LH, the concentration maps show that a substantial widening of the entire length of the transition zone occurred during the penetration of the saltwater wedge, while it remained

relatively thin in the base case. Laboratory observations show that the saltwater upconing mechanism started about 50 minutes after changing the abstraction rate, whereby low-concentration saline water started to reach the well. The final stage of the upconing wedge occurred within 120 min, after which no changes could be observed. The thickness of the transition zone was visibly reduced, albeit it remained slightly wider than in the base case.

These results show that the landward penetration of the saltwater was considerably slower in case LH, even if the pumping rate in case LH was greater. The salinisation of the pumping well was significantly delayed in case LH, which implies that the presence of the top low-K layer improved the capability of the subsurface dam to protect freshwater abstraction. This may be because of the increased freshwater flow below the low-k layer, which exerts more resistance to the salt intrusion in case LH than in the base case. In such conditions, the building up of the saltwater on the seaward side of the subsurface dam is impeded, thereby reinforcing the ability of the subsurface dam to restrict the spillage and penetration of saltwater compared to the base case, even with a higher abstraction rate.

The noticeable widening of the transition zone observed in case LH probably occurred as a result of stronger dispersion along the interface associated with the increased freshwater flow velocity in the lower part of the system. The increased freshwater flow caused more resistance to the density-contrast effects driving the intrusion, as observed by Abdoulhalik and Ahmed (2017b).

3.1.2. Receding-wedge phase: Pumping shut-off

After switching off the pump, the sudden increase of the freshwater flow induced an abrupt repulsion of the saltwater back to the seaside boundary, and the transition zone retrieved its natural, relatively straight shape (Figure 7). Figure 7 shows that the toe of the saltwater wedge migrated faster towards the seaward boundary in the case LH compared to the base case. This result suggests that the decay process of the upconing saltwater wedge that follows the

interruption of pumping would be faster in the presence of the top low K layer, which implies a faster restoration of salinised aquifers. A transition zone widening was observed throughout the retreat in both cases, albeit substantially more pronounced in case LH.

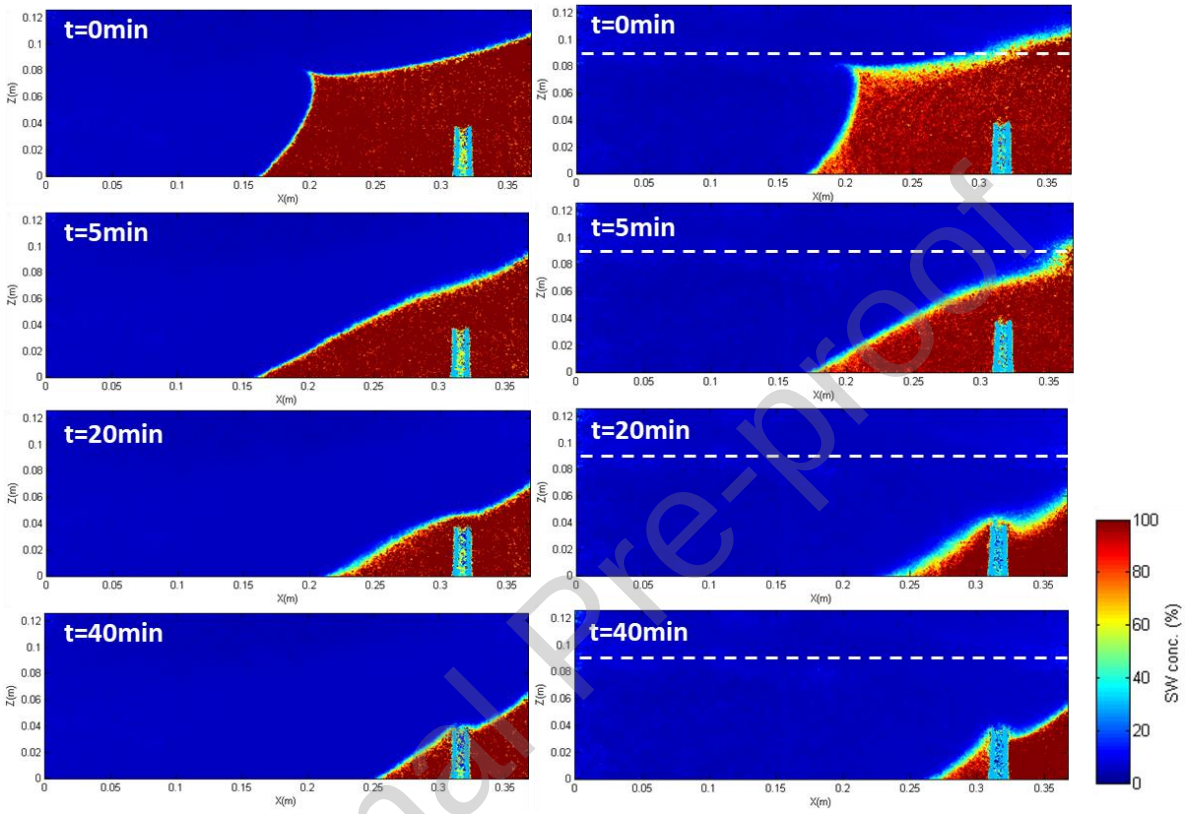

Figure 7: Concentration colour map of the transient **experimental** receding saltwater wedge after turning off the pumping in the base case (left) and case LH (right). The dashed line represents the lower boundary of the low-K layer.

The transition zone widening was associated with the rapid increase of the freshwater flow, which lifted saline water back over the seaward side of the dam. This is due to the excessive dispersion and diffusion occurring along the freshwater-saltwater interface.

The saltwater wedge on the landward side of the wall became relatively steady after some time, forming a smaller residual wedge. The freshwater zone on the landward side of the dam was regarded as cleaned up from contamination when no saline water could be observed, even at a small concentration. The time required for the residual seawater to be completely flushed out from the freshwater zone was estimated at 270 min in the homogeneous case and 220 min in the case LH. This means the homogeneous aquifer needed 23% longer time than the layered

aquifer for desalination and cleanup. The presence of an overlaying low-K layer in the upper part of the aquifer helped reduce the time needed for the residual saline water to be flushed back over the wall. The presence of a low k layer at the top of the aquifer is associated with two opposing influential factors. The first is the downward increased flow velocity in the lower part of the system that facilitates lifting saline water. The second is the reduction of the overall freshwater inflow, which reduces the seaward hydraulic forces needed to flush the denser liquid back over the wall. This result shows that in this configuration, the first factor has more impact on the ability of the subsurface dam to clean up residual saline water from the landward freshwater area.

3.2. Numerical modelling

3.2.1. Validation of the Pumping Condition

Numerical modelling was conducted to simulate the two experimental cases. The numerical validation was done by qualitatively comparing the saltwater wedge shape at the various stages developed by increasing the pumping rate.

Figure 8a shows that the numerical model accurately reproduced the shape of the seawater wedge at a steady state throughout the different phases of the base case. The numerical model confirms the ability of the subsurface dam to retain saline water for Q_1=0.09 mL/s, while spillage occurs after applying Q_2=0.19 mL/s, which agrees with the experimental observations. The model could reproduce the outward curving of the freshwater-saltwater transition zone caused by the pumping as the system reached a steady state, as observed in the physical experiment. After increasing the abstraction rate to Q_3=0.29 mL/s, the saltwater upconing time was well predicted in the numerical model, whereby the saline water reached the well after 30 minutes in the experimental model against t = 35 in the numerical model. The saltwater wedge shape was relatively well reproduced at the final stage of the upconing. Some minor discrepancies could nonetheless be observed in the front of the upconing wedge, which appears

slightly more curved in the numerical model. These slight differences in the upconing time and the shape of the wedge, between the numerical and experimental, are mainly attributed to several factors. Although every effort is made during the experimental setup to produce a homogeneous aquifer by placing the beads on stages and compacting them evenly, yet some small heterogeneities may inevitably exist. This is also the case for each layer in the layered scanrios. Also the laboratory temperature may change which may have slight effects on the visicosity and density of both seawater and freshwater. These factors are not accounted for in the numerical model.

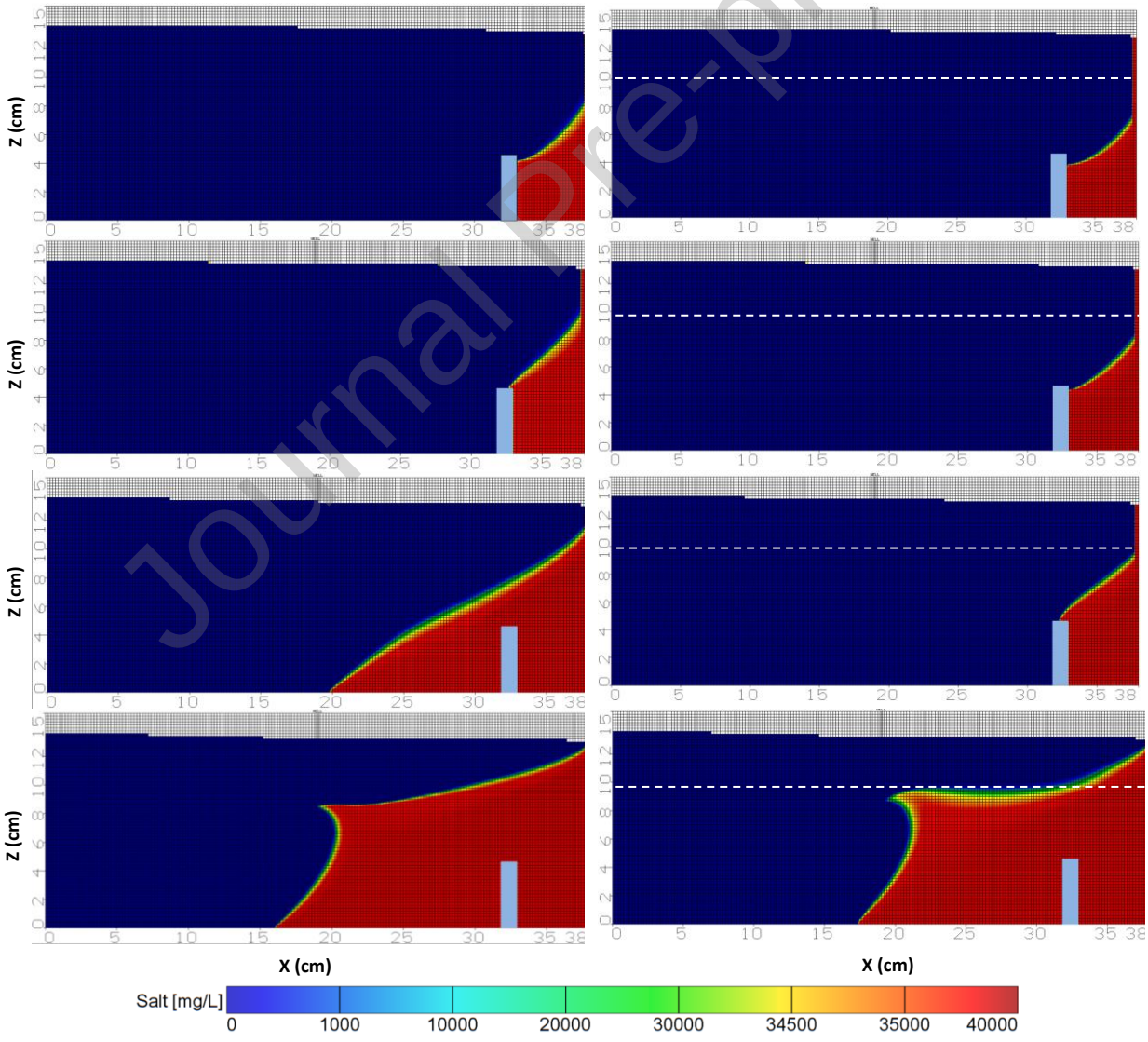

Figure 8. Comparison between base case (left) and case LH (right) for **numerical** saltwater upconing process

Figure 8b shows the numerical data results for the advancing-wedge phase in case LH. The numerical results matched the laboratory data in all the simulated cases. This provides further confirmation of the subsurface dam to retain the seawater on the seaward side of the dam for Q_1=0.09 mL/s and Q_2=0.19 mL/s, although some discrepancy in the height of the saltwater wedge along the boundary, which was slightly overestimated in the numerical model. The model predicted the spillage of saltwater following the application of Q_3=0.29 mL/s, which agrees with the experimental observations. The saltwater upconing time was nonetheless overestimated in the numerical model, i.e., the saline water reached the well noticeably faster in the experimental than in the numerical model.

In contrast, the process was relatively slow in the physical experiments. The estimated time of upconing after establishing Q_3=0.29 mL/s was t = 120 min in the experimental model against t = 130 in the numerical model. These confirm that the upper low K layer improved the ability of subsurface dams to protect freshwater abstraction.

3.2.2. Validation of the Pumping Shut-off

The well pumping was turned off in the base case, which subsequently caused a sharp decrease in the saltwater wedge and increased the freshwater flow towards the seaside. The transient early stage of the saltwater receding wedge is presented in Figure 9 (left). The saltwater wedge receding phase was initiated by turning off the pumping well. Moreover, the interruption of abstraction is followed by rapid movement in the tip of the saltwater cone away from the well towards the seaside with an increase in the freshwater-saltwater interface.

Figure 9 (right) shows the case LH, where the saltwater repulsion wedge towards the seaside was faster than the base case. Retreat in the transition zone area widened in both cases, but the case LH was more pronounced. Also, the toe of SWI was moved towards the sea faster in case LH than in the base case. This concluded that the effect of the presence of the top low K layer

is positive for the interruption of pumping to decay of the upconing saltwater wedge and a faster restoration of salinised aquifers.

The time required for the complete removal of saline water the numerical model yielded was a good match with the experimental results in all the cases investigated here. The numerical results show that the residual saline water was completely removed from the landward side of the dam in less time in both cases. In the homogeneous case, the estimated clean-up time after switching off the pump was t=270 min against t=280 in the numerical model. In case LH, the clean-up time was about t=220 min after switching off the pump, against t=230 min in numerical results. The numerical results nonetheless confirm the positive impact of the overlaying low-permeability layer in lowering the time required to clean up the freshwater zone, which agrees with the laboratory experimental results. These observations demonstrate that the presence of an upper low-permeability layer on the aquifer improved the ability of the subsurface dams to clean up coastal aquifers contaminated by seawater intrusion.

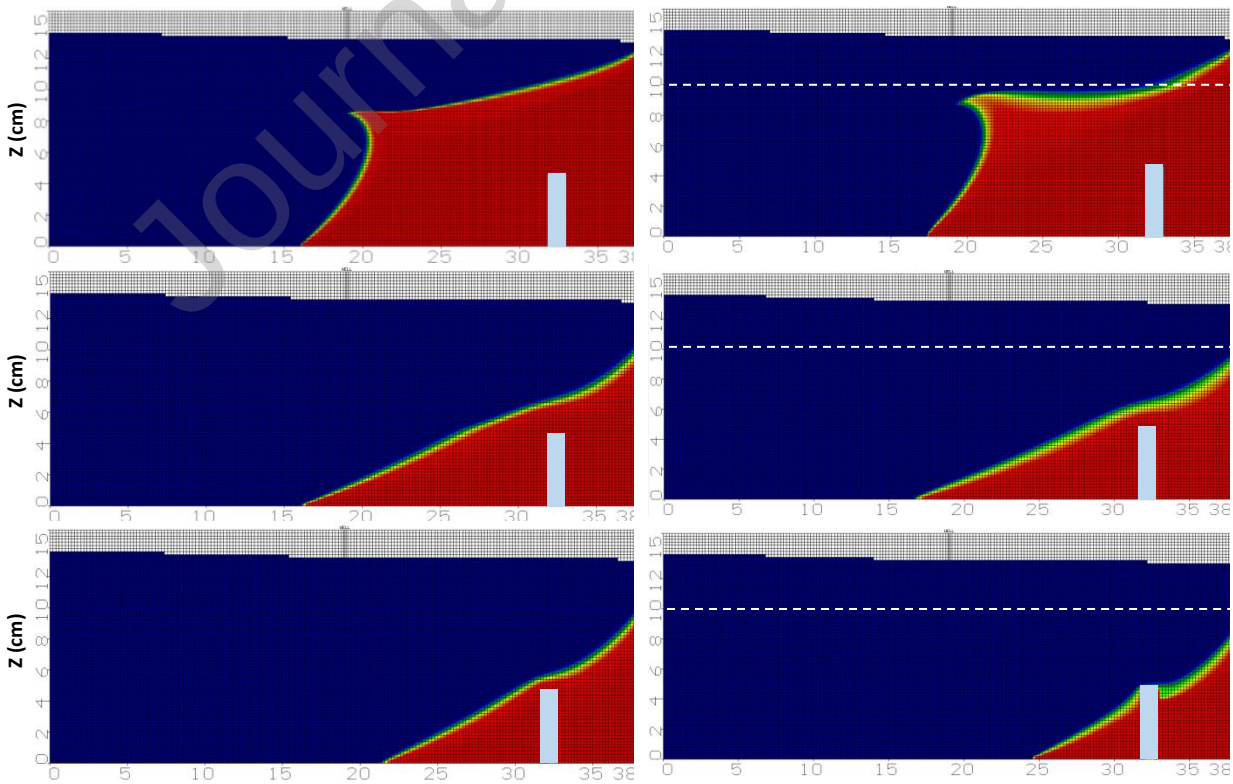

Journal Pre-proof

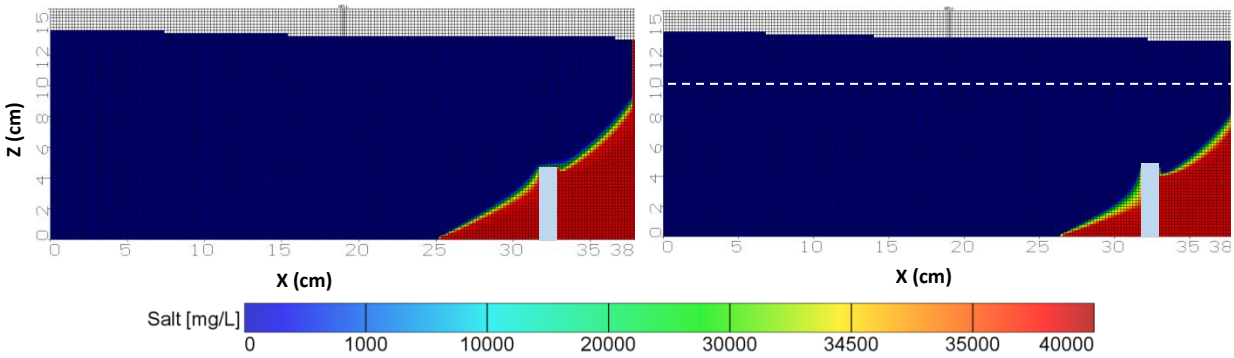

Figure 9. Comparison between base case (left) and case LH (right) **numerical** receding saltwater wedge after turning off the pumping in the base case (left) and case LH (right)

3.3 Other layered cases

The subsurface dam was examined for other two layered aquifer settings. The first is a low K middle layer (case HLH) with a thickness of 45 mm and hydraulic conductivity of 36 cm/min, Figure 10 (left). The second scenario involved a low k layer at the bottom of the aquifer (case HL) with a thickness 45 mm and hydraulic conductivity 36 cm/min, Figure 10 (right). In both configurations, the main aquifer has a hydraulic conductivity of 108 cm/min, the same as the base case.

For case HLH and case HL, the wedge did not spill over the dam wall before the start of the well abstraction (Fig. 10a), which is a similar result to case LH. The dam was able to retain the seawater wedge on the seaside of the wall. For case HLH, the seawater wedge did not even reach the crest of the dam wall, which means the dam can retain the seawater wedge better for this case.

Like the previous cases, Q1 and Q2 were not enough for the wedge to reach the well and contaminate it. The well abstraction increased to Q3=0.29 mL/s, which incited the SWI wedge to move further and reach the well. It took 155 minutes and 190 minutes for the seawater to reach the well for cases HLH and HL, respectively. This is compared with 25 min for the homogenous case and 120 min for case LH for the upconing to occur.

Journal Pre-proof

The results suggest that the existence of a low-K layer has generally delayed the upconing, and it took longer for the SWI to reach and contaminate the abstraction well. In particular, a low permeability layer at the middle or bottom of the aquifer helped delay the SWI wedge from moving towards the abstraction well. These are encouraging results because most real-world aquifers are heterogeneous, which means delayed upconing and safer freshwater abstraction before the SWI reaches the well.

After switching off the pump, the estimated cleanup time was 280 min for case HLH and 410 min for case HL. The low-K layer at the bottom of the aquifer has significantly delayed the cleanup process, as the SWI will be pushed back very slowly in this layer due to the low velocity of the freshwater there. Case LH achieved the quickest cleanup time compared to all other cases. This is obviously due to the greater freshwater velocity in the bottom layer of the aquifer in this scenario, which helps repulse the seawater and push it back to the seaside of the wall. The current results agree with Abdoulhalik and Ahmed (2017a,b), who observed delayed cleanup of up to 50% longer for the case when a low-K layer existed at the bottom of the aquifer compared with the homogeneous case. This low-K bottom layer weakened the resistance to the SWI wedge and prolonged the cleanup process. Table 2 summarises the time needed for the well to be contaminated for all the aquifer configurations examined here.

Table 2: Time for SWI to reach the well and the cleanup time after the pump is off.

Location of the low-K layer	Time for SWI to reach the well (minutes)	Cleanup time after pump is off (minutes)
None (the homogeneous case)	25	280
Top of the aquifer	125	230
Middle of the aquifer	155	280
Bottom of the aquifer	190	410

Journal Pre-proof

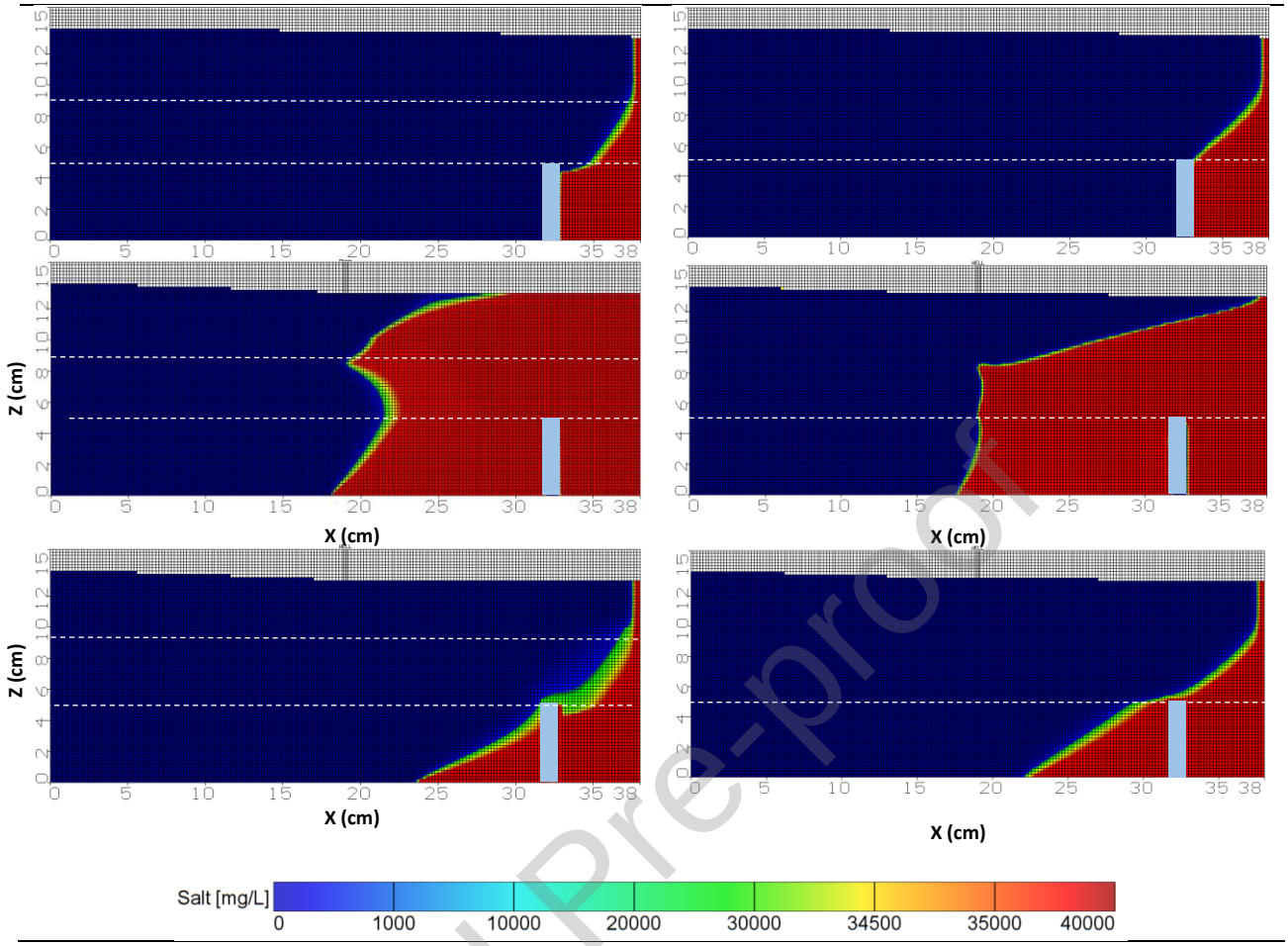

Figure 10. Comparison between concentration colour map of the transient **numerical** saltwater wedge under layered aquifer conditions in the middle layer low K case (left) and bottom layer low K case (right)

4. Discussion

The experimental results provide comprehensive insights into the dynamic behaviour of saltwater wedges under varying pumping rates and aquifer structures. Two experimental scenarios were considered: a homogeneous aquifer (base case) and a layered aquifer with a top low-permeability layer (case LH). Initially, a saltwater wedge formed on the seaward side of the dam in both setups, establishing a steady-state interface without spilling over the subsurface dam.

When pumping began at Q1 = 0.09 mL/s, both cases demonstrated increased saline buildup on the seaward side, but no saltwater spillage occurred landward. Notably, in case LH, the saltwater wedge did not reach the top of the wall, emphasising the role of the low-K layer in repulsing the saltwater wedge and delaying it from spilling over the wall into the landward side

Journal Pre-proof

of the dam. Upon increasing the pumping rate to Q2 = 0.19 mL/s, spillage occurred in the homogeneous case within 5 minutes, whereas case LH remained stable, showing the superior protective effect of the layered system. This can be mainly attributed to the greater freshwater flow in case LH (Abdoulhalik et al. 2022b). The existence of the low-K top layer has pushed the freshwater to mainly flow through the bottom layer, which increased its velocity, and this helped repluse the seawater wedge back to the seaward side of the dam.

Further increasing the abstraction rate to Q3 = 0.29 mL/s triggered saltwater upconing in the homogeneous case after 20 minutes, reaching a steady state at 25 minutes. For case LH, this high pumping rate finally prompted spillage over the dam within five minutes, but still safe to abstract more freshwater from the well. Even under such a condition, upconing in case LH took 50 minutes to be initiated, and it took 120 minutes to reach the well. The wider transition zone in case LH suggests more substantial hydrodynamic dispersion driven by increased freshwater flow at the bottom, thereby impeding saltwater intrusion.

Once the pumping was shut off, both systems transitioned into a receding phase. A rapid freshwater rebound pushed the saline wedge back towards the sea. The saltwater wedge retreated in both homogeneous and LH cases, but the rate was significantly faster in case LH, indicating a quicker aquifer recovery. The transition zone widened in both cases during this retreat, but the widening was more pronounced in the layered case, which experienced a faster re-stabilisation. Case LH showed a cleanup time of 220 minutes, compared to 270 minutes in the homogeneous case, highlighting a 23% faster recovery due to the presence of the upper low-K layer. The likely reason for this faster retreat is the concentration of freshwater velocity in the lower portion of the aquifer, increasing the pushback against the denser saline water.

The other two layered cases, where the low-K layer was at the middle or bottom of the aquifer, showed greater time for the aquifer to be cleaned. It took 155 minutes and 190

Journal Pre-proof

minutes for the seawater to reach the well for cases HLH and HL, respectively. This is compared with 25 minutes for the homogeneous case and 120 minutes for case LH for the upconing to occur. The cleanup time during the seawater wedge retreat was also significantly high in these layered scenarios, especially when the low-K existed at the bottom of the aquifer. These results are in agreement with Aboulhalik and Ahmed (2017a,b), who found that a low-K layer at the bottom of the aquifer weakened the ability of cutoff walls and subsurface dams to control seawater intrusion. Although these studies did not investigate the effectiveness of the wall or dam during freshwater abstractions, the flow dynamics seem to be similar to those observed here, where a well abstraction is considered.

The time delay for the SWI wedge to reach the well in the two cases when the low-K layer existed at the middle and bottom of the aquifer can be attributed to the buoyancy force, which is one of the main drivers of the SWI progression inland. This buoyancy force is weakened in these two aquifer settings as the SWI wedge finds it harder to progress through the low-K layer, where it finds some resistance. Even though the hydraulic gradient has increased due to pumping, the smaller buoyancy force delays the wedge from reaching the well.

5. Summary and conclusions

The effect of a low-K layer on the ability of subsurface dams to protect freshwater abstraction was investigated in a laboratory flow tank. Two laboratory experimental scenarios were examined, including a homogeneous scenario and a scenario where a low-K layer was simulated in the upper part of the aquifer. Automated image analysis was used to accurately depict the salt concentration in the aquifer, thus clearly visualising the saltwater upconing mechanism. The SEAWAT code was used to validate and examine other layered scenarios related to the upconing process. The main findings of the study could be summarised as follows:

Journal Pre-proof

- For equivalent pumping rate increments, the pumping rate required to prompt spillage of the saline water over the subsurface dam was higher in the layered cases compared with the homogeneous aquifer. For the case tested here, the layered aquifer needed 52% more pumping than the base case for the wedge to spill over the dam into the landside.
- The results suggest that the low-K layer enhanced the subsurface dam's ability to obstruct the SWI, thereby allowing for more optimal freshwater abstraction without enabling saltwater to spill over the wall. Fortunately, most real-world aquifers are heterogeneous, meaning the SWI will take longer to reach the freshwater wells.
- The cleanup time was substantially reduced in the presence of a top low-K layer. For the aquifer configurations tested here, it took about 23% less time to clean up an aquifer with a top low-K layer than a homogeneous aquifer or an aquifer with a middle low-K layer.
- The existence of a low-K layer at the bottom of the aquifer significantly prolonged the cleanup process compared to the homogeneous and other layered cases. This aquifer configuration took about 50% longer compared to the homogeneous case and the case with a low-K middle layer, and about 85% longer compared to the case when the low-K layer existed at the top of the aquifer.

The limitation of the study is that the results are mainly based on laboratory experimental and numerical investigations. However, more work is still needed, especially with real field sites affected by seawater intrusion. Yet, the findings of this study highlighted the importance of considering geological heterogeneity and freshwater pumping conditions in designing and implementing subsurface dams to effectively control SWI and protect groundwater resources in coastal areas. The results presented here provide important insights into aquifer layered cases, where subsurface dams are more effective in repulsing

Journal Pre-proof

seawater intrusion than other control measures. This is very important in water resources planning, particularly in coastal areas.

Acknowledgements

The authors wish to thank Queen's University Belfast for providing the facilities for A. Ahmed to conduct the experiments while he was associated with them.

Author credits

Antoifi Abdoulhalik: Writing – original draft, Formal analysis, Conceptualisation.

Ashraf A Ahmed: Conceptualization, Writing – original draft , Supervision, Writing – review & editing.

Ismail Abd-Elaty: Software, Validation.

Conflicts of interest/Competing interests

(The authors declare no conflict of interest.)

Journal Pre-proof

References

1 Abd-Elaty, I., Kuriqi, A., Pugliese, L. and Ahmed, A., 2024. Shoreline subsurface dams to protect coastal aquifers from sea level rise and saltwater intrusion. Applied Water Science, 14(3), pp.1-12.

2 Abdelgawad, A. M., Abdoulhalik, A., Ahmed, A., Moutari, S., and Hamill, G. A., 2018. Transient Investigation of the Critical Abstraction Rates in Coastal Aquifers : Numerical and Experimental Study. Water Resour. Manage. 32, 3563–3577. https://doi.org/10.1007/s11269-018-1988-3

3 Abdoulhalik, A., and Ahmed, A. A., 2024, Abd Elaty, I. Effects of layered heterogeneity on mixed physical barrier performance to prevent seawater intrusion in coastal aquifers. J of Hydrol. https://doi.org/10.1016/j.jhydrol.2024.131343

4 Abdoulhalik, A., Ahmed, A.A., 2018. Transient investigation of saltwater upconing in laboratory-scale coastal aquifer. Estuar. Coast. Shelf Sci. 214 (June), 149–160. https://doi.org/10.1016/j.ecss.2018.09.024.

5 Abdoulhalik, A., and Ahmed, A. A., 2017a. The effectiveness of cutoff walls to control saltwater intrusion in multi-layered coastal aquifers: Experimental and numerical study. J. Environ. Manage. 199, 62–73. https://doi.org/10.1016/j.jenvman.2017.05.040

6 Abdoulhalik, A., and Ahmed, A. A. 2017b. How does layered heterogeneity affect the ability of subsurface dams to clean up coastal aquifers contaminated with seawater intrusion? J. Hydrol., 553, 708–721. https://doi.org/10.1016/j.jhydrol.2017.08.044

7 Abdoulhalik, A., Abdelgawad, A. M., Ahmed, A. A., Moutari, S., & Hamill, G. (2022a). Assessing the protective effect of cutoff walls on groundwater pumping against saltwater upconing in coastal aquifers. Journal of Environmental Management, 323, 116200.

8 Abdoulhalik, A., Ahmed, A., Abdelgawad, A., & Hamill, G. 2022b. The impact of a low-permeability upper layer on transient seawater intrusion in coastal aquifers. Journal of Environmental Management, 307, 114602.

9 Christelis, V. and Mantoglou, A., 2019. Pumping optimization of coastal aquifers using seawater intrusion models of variable-fidelity and evolutionary algorithms. Water resources management, 33(2), pp.555-568.

10 Ebeling, P., Händel, F. and Walther, M., 2019. Potential of mixed hydraulic barriers to remediate seawater intrusion. Science of the total environment, 693, p.133478.

11 Edition, F., 2011. Guidelines for drinking-water quality. *WHO chronicle*, *38*(4), pp.104-8.

12 Fang, Y., Zheng, T., Wang, H., Guan, R., Zheng, X., & Walther, M. 2021. Experimental and numerical evidence on the influence of tidal activity on the effectiveness of subsurface dams. Journal of Hydrology, 603, 127149.

Journal Pre-proof

13 Guo, W. and Langevin, C.D., 2002. User's guide to SEAWAT: a computer program for simulation of three-dimensional variable-density ground-water flow (Vol. 1, No. 434). US Geological Survey.

14 Ketabchi, H., Mahmoodzadeh, D., Ataie-Ashtiani, B. and Simmons, C.T., 2016. Sea-level rise impacts on seawater intrusion in coastal aquifers: Review and integration. Journal of Hydrology, 535, pp.235-255.

15 Kaleris, V. K., and Ziogas, A. I., 2013. The effect of cutoff walls on saltwater intrusion and groundwater extraction in coastal aquifers. J. Hydrol., 476, 370–383. https://doi.org/10.1016/j.jhydrol.2012.11.007

16 Luyun, R., Momii, K., and Nakagawa, K. 2011. Effects of Recharge Wells and Flow Barriers on Seawater Intrusion. Ground Water, 49, 239–249. https://doi.org/10.1111/j.1745-6584.2010.00719.x

17 Pool, M., and Carrera, J., 2010. Dynamics of negative hydraulic barriers to prevent seawater intrusion, Hydrogeol. J., 18, 95–105. https://doi.org/10.1007/s10040-009-0516-1

18 Robinson, G., Ahmed, A.A. and Hamill, G.A., 2016. Experimental saltwater intrusion in coastal aquifers using automated image analysis: Applications to homogeneous aquifers. *Journal of Hydrology*, *538*, pp.304-313.

19 Shi, L., Lu, C., Ye, Y., Xie, Y. and Wu, J., 2020. Evaluation of the performance of multiple-well hydraulic barriers on enhancing groundwater extraction in a coastal aquifer. *Advances in Water Resources*, *144*, p.103704.

20 Stevanović, Z., 2016. Damming underground flow to enhance recharge of karst aquifers in the arid and semi-arid worlds. Environmental Earth Sciences, 75, pp.1-14.

21 Strack, O.D.L., Stoeckl, L., Damm, K., Houben, G., Ausk, B.K. and De Lange, W.J., 2016. Reduction of saltwater intrusion by modifying hydraulic conductivity. *Water Resources Research*, *52*(9), pp.6978-6988.

22 Voss, C.I. and Souza, W.R., 1987. Variable density flow and solute transport simulation of regional aquifers containing a narrow freshwater-saltwater transition zone. Water Resources Research, 23(10), pp.1851-1866.

23 Werner, A.D., Bakker, M., Post, V.E.A., Vandenbohede, A., Lu, C., Ataie-Ashtiani, B., Simmons, C.T., Barry, D.A., 2013. Seawater intrusion processes, investigation and

management: recent advances and future challenges. Adv. Water Resour. 51, 3–26. https://doi.org/10.1016/j.advwatres.2012.03.004

24 Yu, X., Xin, P., Lu, C., 2019. Seawater intrusion and retreat in tidally-affected unconfined aquifers: Laboratory experiments and numerical simulations. Adv. Water Resour. 132, 103393. https://doi.org/10.1016/j.advwatres.2019.103393

25 Zang, Y., Yu, B., Jiang, Y., Shang, C., Lian, X. and Jia, Y., 2023. A simulation-optimization integrated framework for subsurface air barrier strategies to mitigate seawater intrusion in a 3D coastal aquifer. Journal of Hydrology, 626, p.130307.

26 Zang, Y. and Li, M., 2021. Numerical assessment of compressed air injection for mitigating seawater intrusion in a coastal unconfined aquifer. Journal of Hydrology, 595, p.125964.

27 Zheng C, Wang PP, 1999. MT3DMS: a modular three-dimensional multispecies transport model for simulation of advection, dispersion, and chemical reactions of contaminants in groundwater systems; documentation and user's guide.

28 Zheng, T., Yuan, F., Gao, S., Zheng, X., Liu, T., & Luo, J. (2023). The impact of hydraulic conductivity anisotropy on the effectiveness of subsurface dam. Journal of Hydrology, 626, 130360.

Declaration of Competing Interest

The authors declare that they have no known competing financial interests or personal relationships that could have appeared to influence the work reported in this paper.

Journal Pre-proof